J Mol Med
DOI 10.1007/s00109-012-0968-y

JMolMed

ORIGINAL ARTICLE

TRAIL death receptor 4 signaling via lysosome fusion and membrane raft clustering in coronary arterial endothelial cells: evidence from ASM knockout mice

Xiang Li · Wei-Qing Han · Krishna M. Boini · Min Xia · Yang Zhang · Pin-Lan Li

Received: 12 August 2012 / Revised: 29 September 2012 / Accepted: 8 October 2012

Abstract Tumor necrosis factor-related apoptosis-inducing ligand (TRAIL) and its receptor, death receptor 4 (DR4), have been implicated in the development of endothelial dysfunction and atherosclerosis. However, the signaling mechanism mediating DR4 activation leading to endothelial injury remains unclear. We recently demonstrated that ceramide production via hydrolysis of membrane sphingomyelin by acid sphingomyelinase (ASM) results in membrane raft (MR) clustering and the formation of important redox signaling platforms, which play a crucial role in amplifying redox signaling in endothelial cells leading to endothelial dysfunction. The present study aims to investigate whether TRAIL triggers MR clustering via lysosome fusion and ASM activation, thereby conducting transmembrane redox signaling and changing endothelial function. Using confocal microscopy, we found that TRAIL induced MR clustering and co-localized with DR4 in coronary arterial endothelial cells (CAECs) isolated from wild-type (*Smpd1*$^{+/+}$) mice. Furthermore, TRAIL triggered ASM translocation, ceramide production, and NADPH oxidase aggregation in MR clusters in *Smpd1*$^{+/+}$ CAECs, whereas these observations were not found in *Smpd1*$^{-/-}$ CAECs. Moreover, ASM deficiency reduced TRAIL-induced $O_2^{-\cdot}$ production in CAECs and abolished TRAIL-induced impairment on endothelium-dependent vasodilation in small resistance arteries. By measuring fluorescence resonance energy transfer, we found that Lamp-1 (lysosome membrane marker protein) and ganglioside G_{M1} (MR marker) were trafficking together in *Smpd1*$^{+/+}$ CAECs, which was absent in *Smpd1*$^{-/-}$ CAECs. Consistently, fluorescence imaging of living cells with specific lysosome probes demonstrated that TRAIL-induced lysosome fusion with membrane was also absent in *Smpd1*$^{-/-}$ CAECs. Taken together, these results suggest that ASM is essential for TRAIL-induced lysosomal trafficking, membrane fusion and formation of MR redox signaling platforms, which may play an important role in DR4-mediated redox signaling in CAECs and consequently endothelial dysfunction.

Keywords TRAIL · Lysosome fusion · Acid sphingomyelinase · Membrane raft · Endothelial cell · Vasorelaxation

Introduction

The tumor necrosis factor (TNF)-related apoptosis-inducing ligand (TRAIL) is expressed as a type II TNF ligand transmembrane protein which can be released as a vesicle-associated form or a soluble form. Five receptors for TRAIL have been identified. Two death receptors, DR4 and DR5, contain a death domain and transmit an apoptotic signal in response to TRAIL [1]. Two decoy receptors (DcR1 and DcR2) bind TRAIL without activation of the apoptotic machinery and seem to antagonize DR4 and DR5 [2]. Lastly, osteoprotegerin, originally identified as a regulator of osteoclastogenesis, was shown to bind TRAIL and function as a soluble TRAIL receptor [3]. Endothelial cells (ECs) express all TRAIL receptors including DR4 and DR5, and the activation of these receptors has been implicated in the regulation of EC activities including inflammation, proliferation, differentiation, and apoptosis [4–8]. For example, TRAIL down-modulated CCL8 and CXCL10 chemokine expression in human umbilical vein endothelial cells

Xiang Li and Wei-Qing Han contributed equally to this work.

X. Li · W.-Q. Han · K. M. Boini · M. Xia · Y. Zhang (✉) · P.-L. Li (✉)
Department of Pharmacology & Toxicology, Medical College of Virginia Campus, Virginia Commonwealth University, Richmond, VA 23298, USA
e-mail: yzhang3@vcu.edu
e-mail: pli@vcu.edu

Published online: 24 October 2012

(HUVECs), which may contribute to its anti-inflammatory activity by counteracting the ability of TNF-α to promote leukocyte adhesion to ECs [5]. TRAIL induced apoptosis in HUVECs and human dermal and cerebral microvascular ECs [6–8]. In contrast, in HUVECs and human aortic ECs, TRAIL has been shown to activate the Akt and ERK1/2 pathways which may be associated with EC proliferation and differentiation [4]. Thus, these findings indicate that TRAIL may in parallel modulate apoptotic pathways as well as anti-apoptotic/pro-inflammatory pathways in ECs. Although these studies revealed the biological activities of TRAIL on ECs, it remains unknown whether and how this death factor indeed produces endothelial dysfunction when it acts on intact vessels for a short time.

Membrane rafts (MRs, previously as lipid rafts) are dynamic assemblies of cholesterol, lipids with saturated acyl chains, such as sphingolipids and glycosphingolipids, in the exoplasmic leaflet of the membrane bilayer, and cholesterol in the inner leaflet [9]. Recently, accumulating evidence suggest that MR clustering is a novel mechanism mediating and amplifying transmembrane signaling in response to various stimuli in a variety of cell types, including lymphocytes, endothelial cells, and neurons [10–12]. Clustered MRs form membrane signaling platforms, in particular, the ceramide-enriched platforms or macrodomains [9]. These membrane platforms can recruit or aggregate various signaling molecules such as small G proteins, tyrosine kinases, and phosphatases, resulting in the activation of different signaling pathways [9]. More recently, there are increasing evidence that MR clustering on the coronary arterial endothelial cells (CAECs) is an important initiating mechanism in endothelial injury in response to damaging factors such as death receptor agonists, inflammatory factors, and irradiation [9, 11, 13]. It has been shown that MR clustering recruits or aggregates redox signaling molecules such as NADPH oxidase subunits, $gp91^{phox}$, $p47^{phox}$, and Rac GTPase, resulting in the formation of a membrane signal amplification platform that activates and enhance production of $O_2^{-\cdot}$ [11, 14]. These MR signaling platforms associated with $O_2^{-\cdot}$ production have been referred as MR redox signaling platforms. The formation of such MR redox signaling platforms in the EC membrane is associated with ceramide production via lysosomal acid sphingomyelinase (ASM), which is translocated onto the plasma membrane via membrane proximal lysosome trafficking and fusion upon stimulation of death receptors [15–17]. Ceramides spontaneously fuse MRs into large ceramide-enriched membrane domains or platforms, which can serve as MR redox signaling platforms [9, 14]. TRAIL has been demonstrated to stimulate ceramide production through ASM and consequent formation of ceramide-enriched platforms in non-endothelial cells [18]. Based on these observations, the present study hypothesized that TRAIL stimulates $O_2^{-\cdot}$ production through the formation of the MR redox signaling platforms in CAECs, leading to the impairment of endothelium-dependent vasodilation and endothelial injury. We used a series of molecular and physiological approaches to test this hypothesis. Particularly, the roles of ASM in lysosome fusion with the plasma membrane, the formation of MR redox signaling, as well as TRAIL-induced endothelial impairment were examined in primary cultured CAECs and small resistance arteries isolated from ASM-deficient mice, respectively.

Materials and methods

Isolation of mouse coronary arterial endothelial cells

The isolation and the characterization of mouse coronary endothelial cells were performed as described previously [19]. Briefly, the heart was excised with an intact aortic arch and immersed in a Petri dish filled with ice-cold Krebs–Henseleit (KH) solution (in millimolars): 118, NaCl; 1.2, $MgSO_4$; 1.2, KH_2PO_4; 25, $NaHCO_3$; 2.5, $CaCl_2$; and 11, glucose. Surrounding fat and connective tissue were removed from the heart. The cleaned heart with intact aorta was transferred to another Petri dish with fresh KH solution. A 25-gauge needle filled with HBSS (in millimolars: 5.0, KCl; 0.3, KH_2PO_4; 138, NaCl; 4.0, $NaHCO_3$; 0.3, $Na_2HPO_4{\cdot}7H_2O$; 5.6, D-glucose; and 10.0, HEPES; with 2 % antibiotics) was inserted into the aortic lumen opening while the whole heart remained in the ice-cold buffer solution. The opening of the needle was inserted deep into the heart close to the aortic valve. The aorta was tied with the needle as close to the base of the heart as possible. The infusion pump was started with a 20-mL syringe containing warm HBSS at a rate of 0.1 mL/min and the heart was then flushed for 15 min. HBSS was replaced with a warm enzyme solution (1 mg/mL collagenase type I, 0.5 mg/mL soybean trypsin inhibitor, 3 % BSA, and 2 % antibiotic–antimycotic) which was flushed through the heart at a rate of 0.1 mL/min. Perfusion fluid was collected at 30-, 60-, and 90-min intervals. At 90 min, the heart was cut with scissors and the apex was opened to flush out the cells that collected inside the ventricle. The fluid was centrifuged at 1,000 rpm for 10 min, the cell-rich pellets were mixed with the one of the media described below, and the cells were planted in 2 % gelatin-coated six-well plates and incubated in 5 % CO_2–95 % O_2 at 37 °C. Medium 199-F-12 medium (1:1) with 10 % fetal bovine serum (FBS) and 2 % antibiotics was used for isolated endothelial cells. The medium was replaced 3 days after cell isolation and then once or twice each week until the cells grew to confluence. All biochemical studies in the present study were performed using CAECs of two to four passages. CAECs were identified by Dil-Ac-LDL staining

as described previously [19, 20]. Six-week-old male C57BL/6J ASM-deficient (*Smpd1*$^{-/-}$; *Smpd1* is the gene symbol for the ASM gene *sphingomyelin phosphodiesterase 1*) mice and their wild-type littermates (*Smpd1*$^{+/+}$) were used in the present study; mouse genotyping was performed as described previously [21]. All animals were provided standard rodent chow and water ad libitum in a temperature-controlled room. All protocols were approved by the Institutional Animal Care and Use Committee of Virginia Commonwealth University (Richmond, VA).

Immunofluorescent microscopic analysis of MR clusters

CAECs were grown on poly-L-lysine-coated glass coverslips. After fixation with 4 % PFA, cells were incubated with Alexa Fluor 488-conjugated cholera toxin B (Alexa488-CTXB, 2 μg/mL, 2 h; Molecular Probes, Palo Alto, CA), which binds with the MR-enriched ganglioside G_{M1}. For dual-staining detection of the co-localization of MRs with DR4/5, ASM, ceramide, or gp91^{phox}, the cells were first incubated with Alexa488-CTXB and then with anti-DR4 or DR5 (1:250, BD Biosciences, San Jose, CA), anti-ASM (1:200, Santa Cruz, CA), anti-ceramide (1:200, Enzol Life Sciences, Farmingdale, NY), and anti-gp91^{phox} (1:200, BD Biosciences), respectively, which was followed by corresponding Alexa555-conjugated secondary antibodies (1:500, Invitrogen, Grand Island, NY). Then, co-localization was visualized with confocal microscopy. To accurately observe staining on the cell membrane, these cells were not permeabilized by excluding detergent in the washing and incubation buffer (phosphate-buffered saline, PBS). Clustering was defined as one or several intense spots or patches of fluorescence on the cell surface, while unstimulated cells displayed a homogenous distribution of the fluorescence throughout the membrane. The results were given as the percentage of cells showing a cluster as described previously [11, 22].

Electron spin resonance detection of endothelial $O_2^{-\cdot}$

Electron spin resonance was performed as described previously [11]. Gently collected CAECs were suspended in modified Krebs–HEPES buffer (in millimolars): NaCl, 99.01; KCl, 4.69; $CaCl_2$, 1.87; $MgSO_4$, 1.20; K_2HPO_4, 1.03; $NaHCO_3$, 25.0; Na-HEPES, 20.0; and glucose, 11.1; pH 7.4) supplemented with deferoxamine (100 μmol/L, metal chelator). Approximately 1×10^6 cells were then incubated with TRAIL (100 ng/L) for 15 min; these cells were subsequently mixed with 1 mML of the $O_2^{-\cdot}$-specific spin trap 1-hydroxy-3-methoxycarbonyl-2,2,5,5-tetramethylpyrrolidine (CMH) in the presence or absence of manganese-dependent superoxide dismutase (SOD, 500 U/mL; Sigma, St. Louis, MO). The cell mixture was then loaded in glass capillaries and immediately kinetically analyzed for $O_2^{-\cdot}$ production for 10 min. The SOD-inhibited fraction of the signal was compared. The electron spin resonance spectrometry (ESR) settings were as follows: biofield, 3,350; field sweep, 60 G; microwave frequency, 9.78 GHz; microwave power, 20 mW; modulation amplitude, 3 G; 4,096 points of resolution; receiver gain, 100; and kinetic time, 10 min.

Vascular reactivity in in vitro perfused and pressurized small resistance arteries

Small mouse mesenteric arteries (third-order branch from the superior mesenteric artery, ~100 μm) were dissected from 6-week-old mice in ice-cold physiological saline solution (PSS) with the following composition (in millimolars)—NaCl, 119; KCl, 4.7; $CaCl_2$, 1.6; $MgSO_4$, 1.17; NaH_2PO_4, 1.18; $NaHCO_3$, 24; EDTA, 0.026; and glucose, 5.5 (pH 7.4)—and carefully cleaned off of fat and connective tissues under a dissection microscope. The dissected arteries were immediately transferred to a water-jacketed perfusion chamber and cannulated with two glass micropipettes at their in situ length as described previously [23]. The outflow cannula was clamped and the arteries were pressurized to 60 mmHg and equilibrated in PSS at 37 °C. PSS in the bath was continuously bubbled with a gas mixture of 95 % O_2 and 5 % CO_2 throughout the experiment. After a 1-h equilibration period, the arteries were pre-contracted with phenylephrine (PE, 1–10 nM) until an ~50 % of decrease in resting diameter was reached. Once steady-state contraction was obtained, cumulative dose–response curves to the endothelium-dependent vasodilator acetylcholine (10^{-9}–10^{-5} M) were determined by measuring changes in internal diameter. To induce endothelial impairment, small arteries were perfused with TRAIL (100 ng/mL) in the lumen and incubated for 1 h. All other drugs were added into the bath solution unless otherwise indicated. The vasodilator response was expressed as the percent relaxation of PE-induced pre-contraction based on changes in arterial internal diameter. The arteries were excluded from statistical analysis if the contractile response to PE was <40 % or dilator response to acetylcholine was <80 %. Internal arterial diameter was measured with a video system composed of a stereomicroscope (Leica MZ8), a charge-coupled device camera (KP-MI AU, Hitachi), a video monitor (VM-1220U, Hitachi), a video measuring apparatus (VIA-170, Boeckeler Instrument), and a video printer (UP890 MD, Sony). The arterial images were recorded continuously with a videocassette recorder (M-674, Toshiba).

Fluorescence resonance energy transfer analysis

Fluorescein isothiocyanate (FITC)/tetramethyl rhodamine isothiocyanate (TRITC) pairs were used for fluorescence

resonance energy transfer (FRET) assay. CAECs were stained with FITC-conjugated anti-Lamp-1 (a lysosomal marker protein, 1:200; BD Biosciences) and TRITC-labeled CTXB (TRITC-CTXB, 2 μg/mL, 2 h; Molecular Probes) as described above. An acceptor bleaching protocol was used to measure FRET between FITC/TRITC as described previously [22]. Briefly, after the pre-bleaching image was normally taken, the laser intensity at the excitement wavelength of the acceptor (TRITC) was increased from 50 to 98 % and continued to excite the cell sample for 2 min to bleach the acceptor fluorescence. After the intensity of the excitement laser for acceptor was adjusted back to 50 %, the post-bleaching image was taken for FITC. A FRET image was obtained by the subtraction of the pre-bleaching images from the post-bleaching images and given a dark blue color. After measuring the FITC fluorescence intensity of the pre-, post-, and FRET images, FRET efficiency was calculated through the following equation:

$$E = \left(\mathrm{FITC}_{\mathrm{post}} - \mathrm{FITC}_{\mathrm{pre}}\right)/\mathrm{FITC}_{\mathrm{post}} \times 100\%$$

FM1-43 fluorescence quenching

FM1-43 quenching was performed to detect lysosomal fusion to the plasma membrane as described previously [22]. CAECs were firstly loaded with 8 μM FM1-43 (Molecular Probes) for 2 h at 37 °C. After washing with FBS-free medium, a FM1-43 quenching reagent, bromide phenol blue (BPB, 1 mM; Molecular Probes), was added in the extracellular medium. Cells were then stimulated with or without TRAIL and FM1-43 fluorescence scanned under a confocal microscopy (Olympus) with a low-power laser ($\lambda_{\mathrm{excitation}}$= 488 nm) to avoid fluorescent bleaching.

Statistics

Data are presented as the mean±SE. Significant differences between and within multiple groups were examined using ANOVA for repeated measures, followed by Duncan's multiple-range test. Student's t test was used to detect significant differences between two groups. A value of $P<0.05$ was considered statistically significant.

Results

TRAIL induces MR clustering in mouse CAECs

As shown in Fig. 1a, representative MR patches in CAECs under resting control condition and during TRAIL (100 ng/mL, 15 min) stimulation were detected by confocal microscopy. Under the resting condition, there was only a diffuse fluorescent staining on the cell membrane by Alexa488-CTXB (CTXB specifically binds MR marker ganglioside G_{M1}), indicating the possible distribution of single MRs

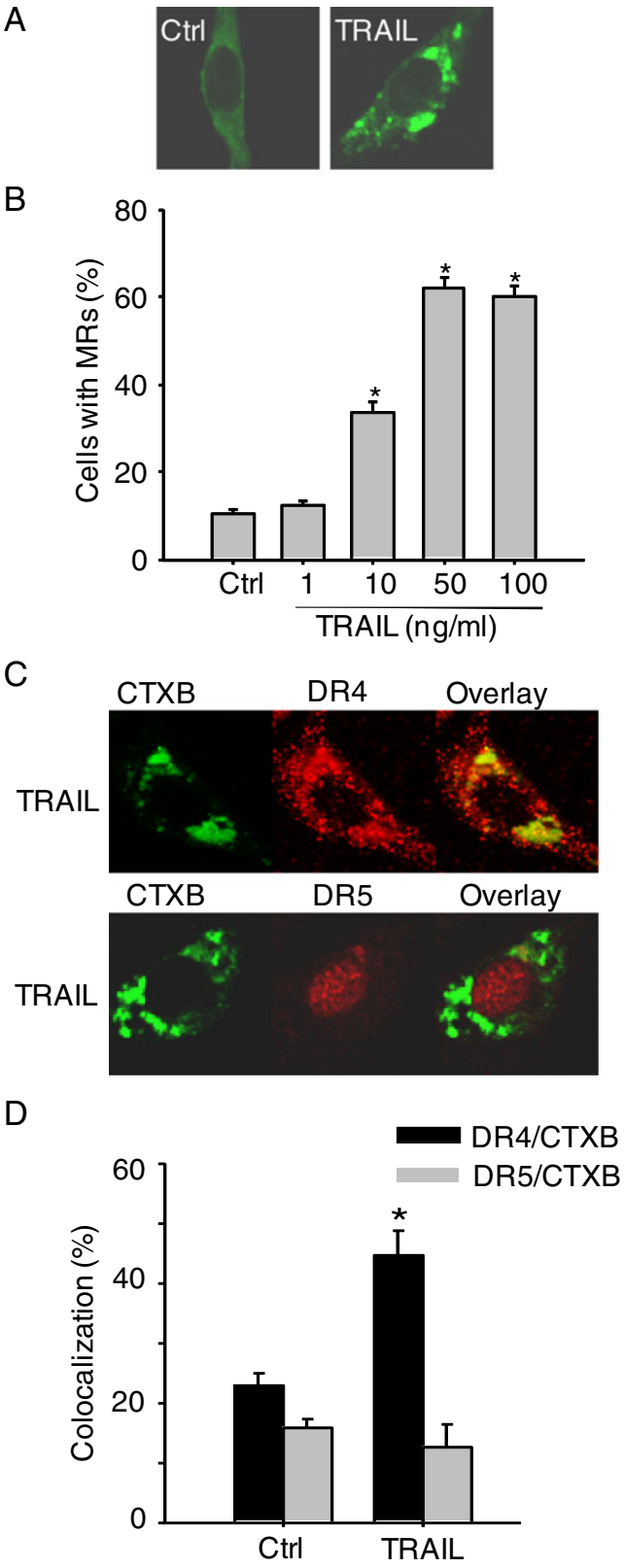

◀ **Fig. 1** TRAIL induces MR clustering in mouse CAECs via DR4 receptor. **a** Representative confocal images showing TRAIL-induced clustering of MR markers ganglioside G_{M1}, which were detected by cholera toxin subunit B (*CTXB*). **b** Summarized data showing the dose-dependent effect of TRAIL (0–100 ng/mL) on MR clustering in *Smpd1*$^{+/+}$ CAECs (n=6). **c** Confocal microscopy of *Smpd1*$^{+/+}$ CAECs revealed a co-localization of DR4, but not DR5, with MR clusters upon TRAIL stimulation. **d** Summarized data showing the co-localization between MRs and DR4 or DR5 in mouse *Smpd1*$^{+/+}$ CAECs. *P<0.05 vs. control (n=6)

without clusters for fluorescent spots or patches. However, when these cells were incubated with TRAIL, large fluorescent dots or patches were detected on the cell membrane. These fluorescent patches indicate the formation of MR clusters or macrodomains. The percentage of cells with intense MR clusters was summarized in Fig. 1b showing that TRAIL dose-dependently increased MR clustering in CAECs. Since the optimum response of MR clustering was observed with 100 ng/mL TRAIL for 15 min, the same treatment was used in all experiments of the present study, if not otherwise mentioned. Figure 1c shows that DR4 co-localized with MR clusters in CAECs upon TRAIL stimulation, as detected by a number of large yellow patches or spots in overlaid image. In contrast, no significant co-localization was observed between the DR5 and MR clusters in CAECs with TRAIL treatment. The percentage of cells with intense yellow patches was summarized in Fig. 1d indicating that DR4, but not DR5, is involved in TRAIL-induced MR clustering in CAECs.

TRAIL triggers ASM translocation and ceramide production in MR clusters

To investigate the spatial relation between MR clusters and ASM or ceramide, CAECs were stimulated with TRAIL and stained with Alexa488-CTX- and Alexa555-conjugated antibodies against ASM or ceramide. As shown in Fig. 2a–d, confocal microscopy revealed that ASM or ceramide co-localized in MR clusters in *Smpd1*$^{+/+}$ CAECs after TRAIL stimulation. However, such TRAIL-induced co-localization of ASM or ceramide with MR clusters was abolished in *Smpd1*$^{-/-}$ CAECs.

TRAIL-induced NADPH oxidase aggregation in MR clusters requires ASM activity

We next investigate whether TRAIL induces the formation of MR redox signaling platforms by examining the aggregation of gp91^{phox} in MR clusters since gp91^{phox} is a major NADPH oxidase subunit in the plasma membrane of CAECs. As shown in Fig. 3a, b, TRAIL increased the co-localization between MRs and gp91^{phox} in *Smpd1*$^{+/+}$ CAECs, whereas TRAIL failed to increase such co-localization in *Smpd1*$^{-/-}$ CAECs.

ASM deficiency reduces TRAIL-induced $O_2^{-\cdot}$ production in CAECs

To further examine whether TRAIL-induced MR redox signaling is mediated via ASM/ceramide, *Smpd1*$^{+/+}$ or *Smpd1*$^{-/-}$ CAECs were stimulated with TRAIL and the $O_2^{-\cdot}$ production in these cells was measured by ESR spectrometric analysis. As shown in Fig. 4, in *Smpd1*$^{+/+}$ CAECs, TRAIL significantly increased $O_2^{-\cdot}$ production by 2.4-fold compared to the control. However, there was no significant increase in $O_2^{-\cdot}$ production observed in *Smpd1*$^{-/-}$ CAECs with TRAIL treatment.

ASM deficiency reverses TRAIL-induced impairment on endothelium-dependent vasodilation in small resistance arteries

The results above demonstrate that TRAIL activates NADPH oxidase-derived $O_2^{-\cdot}$ production via the MR redox signaling pathway. To further investigate the functional significance of TRAIL-induced MR redox signaling, we examined the effects of TRAIL on acetylcholine-induced vasodilation response in small mesentery resistance arteries. As shown in Fig. 5a, acetylcholine produced a concentration-dependent vasorelaxation in *Smpd1*$^{+/+}$ arteries with a maximal response of 86±2.5 % at a concentration of 10^{-5} M. Incubation of these arteries with TRAIL significantly attenuated acetylcholine-induced vasodilation with maximal attenuation of arterial diameters by 40 %. In contrast, TRAIL failed to attenuate the endothelium-dependent vasodilation to acetylcholine in similar arteries isolated from *Smpd1*$^{-/-}$ mice (Fig. 5b).

TRAIL-induced lysosome trafficking to MRs in CAECs is ASM-dependent

We previously reported that lysosome-targeted ASM is able to traffic to and expose to the cell membrane surface, which may lead to MR clustering and NADPH oxidase activation in CAECs in response to various death receptor stimuli such as Fas ligand (FasL) and endostatin [11, 22]. Thus, we tested the hypothesis that TRAIL triggers lysosomal trafficking and fusion with the plasma membrane that is involved in ASM translocation, ceramide production, and MR redox signaling. As shown in Fig. 6a–c, TRAIL significantly increased the FRET (blue images) between FITC-Lamp-1 (lysosome marker) and TRITC-CTXB in *Smpd1*$^{+/+}$ CAECs, but not in *Smpd1*$^{-/-}$ CAECs. As summarized in Fig. 6d, FRET efficiency between FITC-Lamp-1 and TRITC-CTXB was significantly increased in response to TRAIL stimulation in *Smpd1*$^{+/+}$ CAECs; however, such increase in FRET efficiency was not observed in *Smpd1*$^{-/-}$ CAECs.

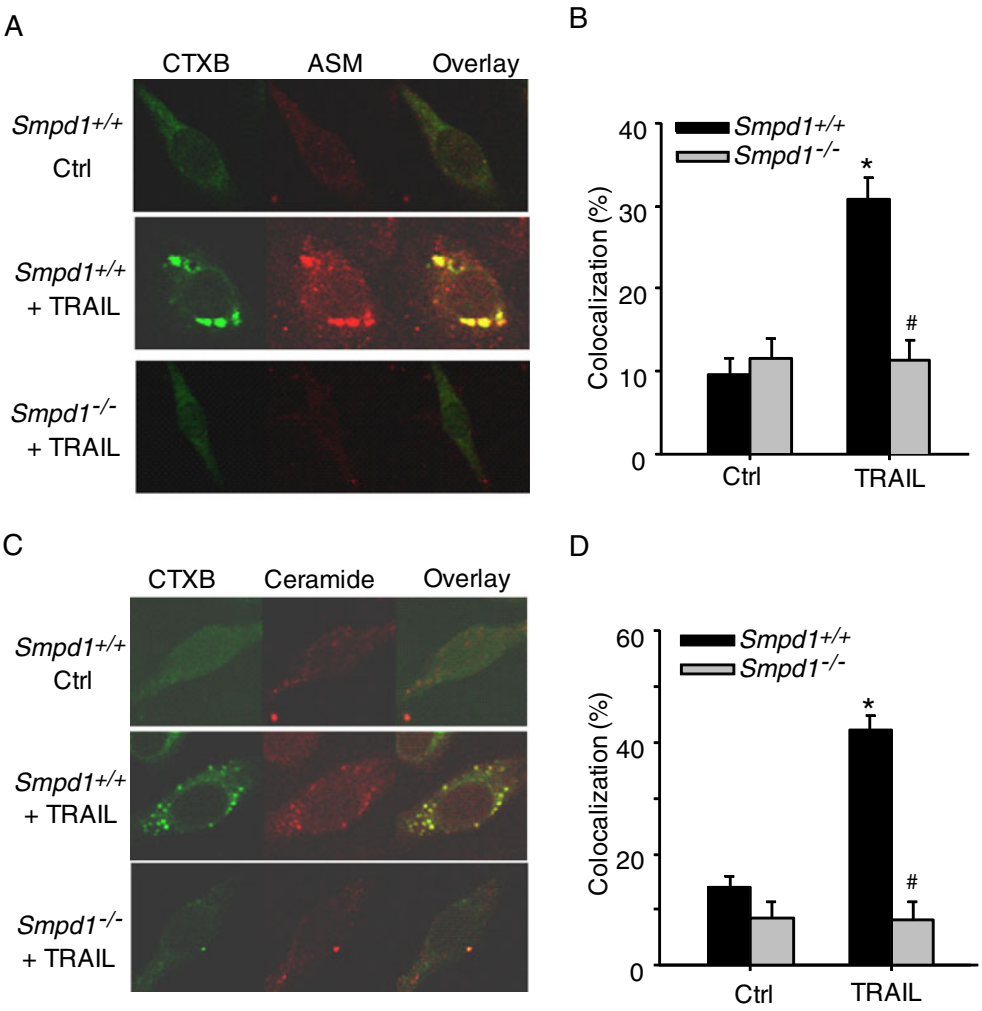

Fig. 2 TRAIL triggers the translocation of ASM to MR domains in mouse CAECs. **a** Representative confocal images depicting the effect of TRAIL on the co-localization between MRs (detected by CTXB) and ASM in *Smpd1*$^{+/+}$ and *Smpd1*$^{-/-}$ CAECs. **b** Displayed are the summarized data showing the co-localization between MRs and ASM. **c** Representative confocal images depicting the effect of TRAIL on the co-localization between MRs and ceramide in *Smpd1*$^{+/+}$ and *Smpd1*$^{-/-}$ CAECs. **d** Displayed are the summarized data showing the co-localization between MRs and ceramide from six independent experiments. **P*<0.05 vs. *Smpd1*$^{+/+}$ control; $^{\#}$*P*<0.05 vs. *Smpd1*$^{+/+}$ TRAIL (*n*=6)

ASM deficiency disrupts TRAIL-induced lysosome fusion with the plasma membrane

We further investigated whether TRAIL-induced lysosomal trafficking to MRs is followed by lysosomal fusion with the plasma membrane and whether ASM is needed for this fusion process. CAECs were loaded with FM1-43, a fluorescence probe accumulated in lysosomes, and then incubated in fresh culture medium containing BPB, which binds FM1-43 and quenches its fluorescence. As shown in Fig. 7a, c, TRAIL induced a significant decrease in FM1-43 fluorescence in *Smpd1*$^{+/+}$ CAECs, indicating that the lysosome fuses with the plasma membrane and exposes its contents to extracellular spaces. However, TRAIL did not decrease FM1-43 in *Smpd1*$^{-/-}$ CAECs (Fig. 7b, c). These results indicated that TRAIL-induced lysosome fusion requires ASM activity.

Discussion

The present study demonstrates that death receptor ligand, TRAIL, triggers MR clustering, the formation of MR redox signaling platforms, the activation of NADPH oxidase, and the production of $O_2^{\cdot-}$ in these platforms in isolated mouse CAECs and induces impairment in endothelium-dependent vasodilation in isolated and pressurized small resistance arteries. In addition, ASM deficiency abolishes these TRAIL-induced signaling events in CAECs and impairment in arteries. These data suggest a novel role of lysosomal ASM-mediated MR redox signaling in the action of TRAIL on ECs and TRAIL-induced endothelial injury.

MR clustering was first visualized on the cell membrane of CAECs by confocal microscopic analysis of CTXB-positive clusters. CTXB relatively specifically binds to MR-enriched ganglioside G_{M1}. The present study demonstrated that TRAIL dose-dependently increased MR clustering in primary cultured CAECs. Our findings are consistent with our previous studies demonstrating that MRs in the EC membrane are evenly distributed and CTXB staining displays a random punctuate staining pattern, whereas stimulation of ECs with death factors including FasL, TNF-α, or endostatin results in the formation of multiple "non-polarized" CTXB-positive patches [11]. Several previous studies also demonstrated that TRAIL can induce MR

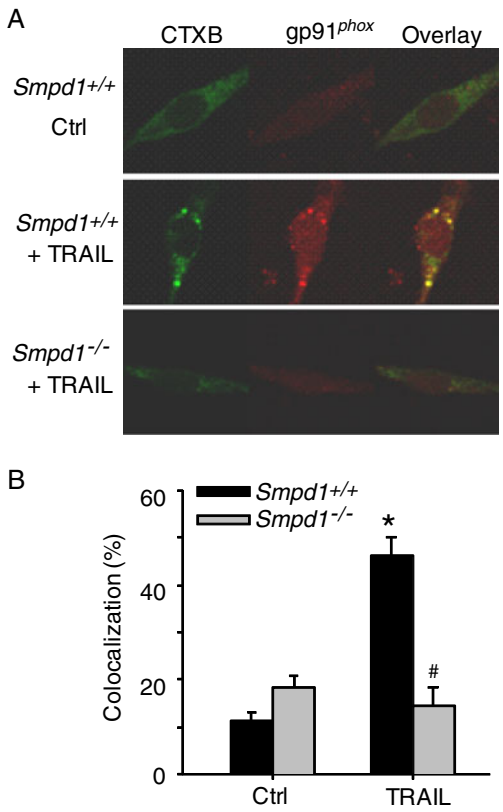

Fig. 3 ASM deficiency abolishes TRAIL-induced clustering of NADPH oxidase subunits gp91^{phox} in MR domains in CAECs. **a** Representative confocal fluorescence images showing the co-localization between MRs and gp91^{phox} in *Smpd1*$^{+/+}$ and *Smpd1*$^{-/-}$ CAECs. **b** Displayed are the summarized data showing the co-localization between MRs and gp91^{phox} from six independent experiments. *P<0.05 vs. *Smpd1*$^{+/+}$ control; $^{\#}P$<0.05 vs. *Smpd1*$^{+/+}$ TRAIL (n=6)

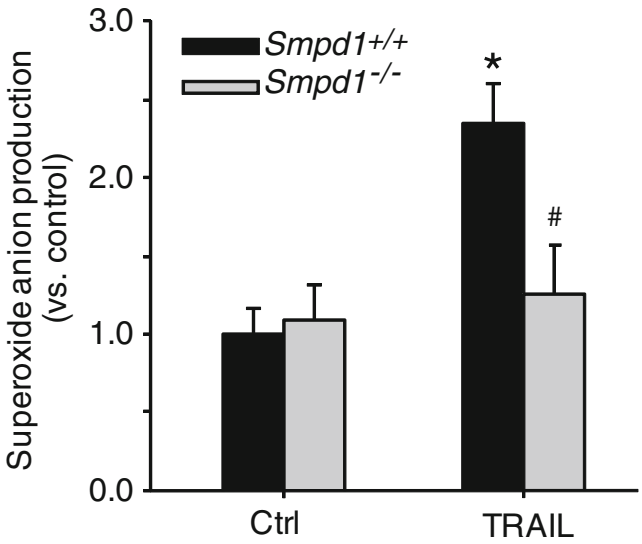

Fig. 4 Reduction of TRAIL-induced $O_2^{\cdot-}$ production in ASM-deficient CAECs. CAECs were stimulated with or without TRAIL and then incubated with $O_2^{\cdot-}$-specific spin trap CMH to form more stable free radicals (CMH–$O_2^{\cdot-}$), which were immediately analyzed by ESR. Summarized data showing the effect of TRAIL on $O_2^{\cdot-}$ production in *Smpd1*$^{+/+}$ and *Smpd1*$^{-/-}$ CAECs. *P<0.05 vs. *Smpd1*$^{+/+}$ control; $^{\#}P$<0.05 vs. *Smpd1*$^{+/+}$ TRAIL (n=6)

clustering in other cell types such as splenocytes and glioblastomas [18, 24, 25]. Together, these findings support the view that MR clustering may serve as a common mechanism for death receptor activation-coupled transmembrane signaling. Despite the presence of both TRAIL receptors DR4 and DR5 in MR microdomains in non-endothelial cells [24, 26, 27], the present study only found DR4, but not DR5, in MR clusters after TRAIL stimulation, implicating that DR4 is activated by TRAIL and involved in consequent MR clustering in CAECs.

Next, we explored the mechanism by which TRAIL stimulates MR clustering. Ceramide spontaneously fuses MR microdomains to larger ceramide-enriched membrane domains. In this regard, ceramide has been proposed as the driving force in promoting MR clustering and subsequent signaling pathway in a variety of mammalian cells [9, 10, 28]. Our previous study has demonstrated that ASM activation serves as a triggering mechanism and driving force leading to the fusion of membrane proximal lysosomes into MR clusters on the cell membrane of CAECs in response to FasL, TNF-α, and endostatin [11, 16, 22]. In addition, TRAIL-induced MR clustering requires ASM–ceramide signaling in non-endothelial cells such as splenocytes and Jurkat leukemia cells [18, 29]. Consistently, the present study found that TRAIL significantly increased the enrichment of ASM and ceramide in the MR clusters, which was almost completely blocked in *Smpd1*$^{-/-}$ CAECs. These results confirm that ASM aggregation and activation in MR clusters are essential to the MR clustering process in CAECs in response to TRAIL. Moreover, our findings further reinforce the concept that ASM activation is a common mechanism mediating MR clustering and corresponding signaling platform formations in ECs, in particular upon death receptor activation.

Increasing evidence suggests that MR clustering is able to promote the aggregation of NADPH oxidase subunits and to form MR redox signaling platforms after death receptor activation [11, 30–32]. By using confocal microscopy, the present study again demonstrated the formation of such MR redox signaling platforms, which were characterized by the aggregation of gp91^{phox} in MR clusters in *Smpd1*$^{+/+}$ CAECs in response to TRAIL activation. Interestingly, in *Smpd1*$^{-/-}$ CAECs, the TRAIL-induced aggregation of NADPH oxidase subunits was abolished. Correspondingly, ESR analysis of $O_2^{\cdot-}$ production also showed that TRAIL-enhanced NADPH oxidase activation in MR clusters was prevented in CAECs with *Smpd1* gene deletion. These results support the

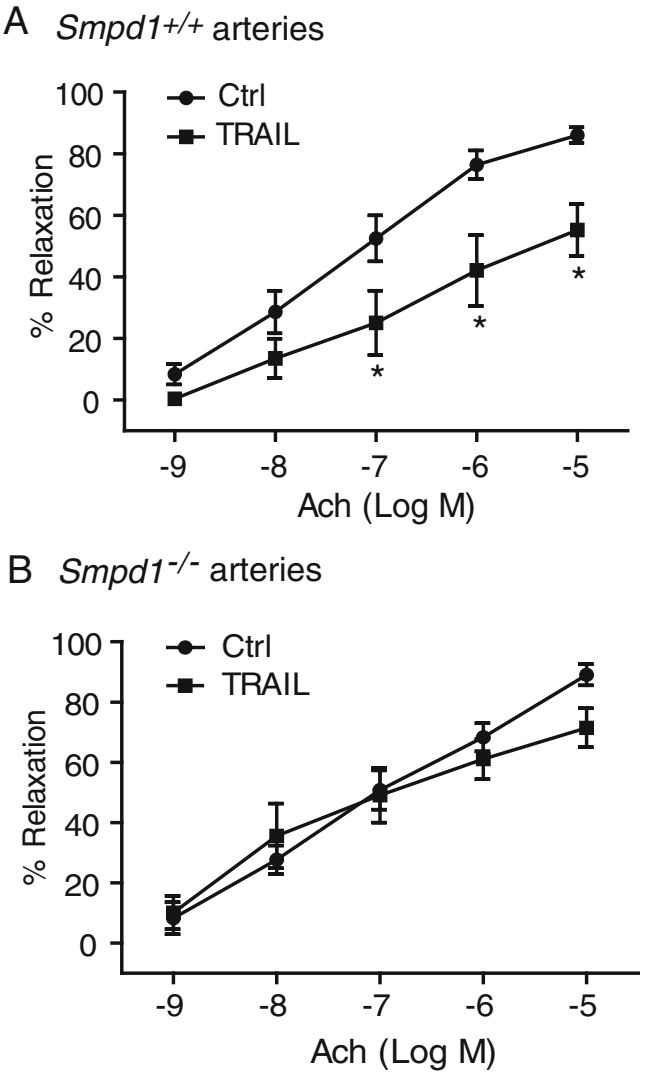

Fig. 5 Effect of TRAIL on the concentration-dependent vasodilator response in freshly isolated and pressurized mouse arteries. **a** Summarized data showing that pretreatment with TRAIL significantly attenuated acetylcholine (*Ach*)-induced endothelium-dependent relaxation in small arteries isolated from *Smpd1*$^{+/+}$ mice. **b** Summarized data showing that pretreatment with TRAIL had no inhibitory effect on Ach-induced endothelium-dependent relaxation in small arteries isolated from *Smpd1*$^{-/-}$ mice. *P<0.05 vs. *Smpd1*$^{+/+}$ control (n=6 mice)

view that in CAECs upon TRAIL stimulation, MR clustering is associated with lysosomal ASM-mediated ceramide production and serves as a driving force to assemble and activate NADPH oxidase on the EC membrane. To our knowledge, the present study, for the first time, reveals that TRAIL triggers lysosomal ASM-mediated MR redox signaling in ECs.

Endothelial dysfunction in small resistance arteries is typically characterized by reduced or loss of endothelium-dependent vasodilation. To this end, the present study demonstrated that TRAIL impairs the endothelium-dependent vasodilator responses in isolated and pressurized small resistance arteries. Our results provide direct evidence that TRAIL produces an early action to induce endothelial dysfunction before detectable apoptotic effect. TRAIL has been reported to induce a detectable apoptosis only with long-term treatment of ECs (>15 h) [33, 34]. Given a relative resistance of ECs to apoptosis, functional impairment may represent one of the most important pathological actions of this apoptotic peptide in ECs. Additionally, TRAIL-induced impairment on vasodilator responses was not observed in ASM-deficient arteries, indicating that this inhibitory action of TRAIL is associated with the lysosomal ASM-mediated formation of MR clusters. Taken together, the results from CAECs and vessel preparation support the view that TRAIL-induced endothelial dysfunction is associated with increased $O_2^{\cdot-}$ production from the lysosomal ASM-mediated formation of MR redox signaling platforms. We also found that acetylcholine-induced vasodilation was attenuated by inhibiting nitric oxide (NO) synthase, suggesting a NO-dependent vasodilation induced by acetylcholine (data not shown). Thus, increased endothelial $O_2^{\cdot-}$ production by TRAIL could reduce the bioavailability of NO, resulting in the impairment of endothelium-dependent vasodilation, as shown in our previous studies and by others [11, 23, 35].

Lysosome trafficking to and fusion with the plasma membrane has been identified as an early signaling event in ECs upon death receptor activation [10, 22]. However, there is no direct evidence showing that ASM is actively involved in this fusion process. To this end, we performed more experiments to directly confirm and compare the fusion of lysosomes to te plasma membrane in *Smpd1*$^{+/+}$ and *Smpd1*$^{-/-}$ CAECs upon TRAIL stimulation. We found that TRAIL caused the co-localization of lysosome marker Lamp-1 with MR clusters on the cell membrane and increased FRET efficiency between MRs and Lamp-1 in *Smpd1*$^{+/+}$ CAECs. Because FRET can only occur between molecules in a distance within a 10-nm range, increased FRET between Lamp-1 and the MR component ganglioside G_{M1} should indicate that some lysosomes are indeed fused into the cell membrane within MR clusters. We also provided direct evidence that TARIL triggers lysosome fusion in living cells using FM1-43, a lysosome-specific fluorescence which can be reversibly quenched by BPB. In the quenching experiments, TRAIL was found to cause a decrease in the FM1-43 fluorescence in *Smpd1*$^{+/+}$ CAECs, which was attributable to TRAIL-stimulated lysosome fusion with the plasma membrane, allowing BPB to enter the lysosomes to quench FM1-43 fluorescence. The TRAIL-induced increase in FRET signals and the decrease in FM1-43 fluorescence were not observed in *Smpd1*$^{-/-}$ CAECs. Thus, all these direct or indirect evidence strongly suggest that the fusion of lysosomes into the cell plasma membrane occurs in these CAECs on TRAIL stimulation and that such TRAIL-

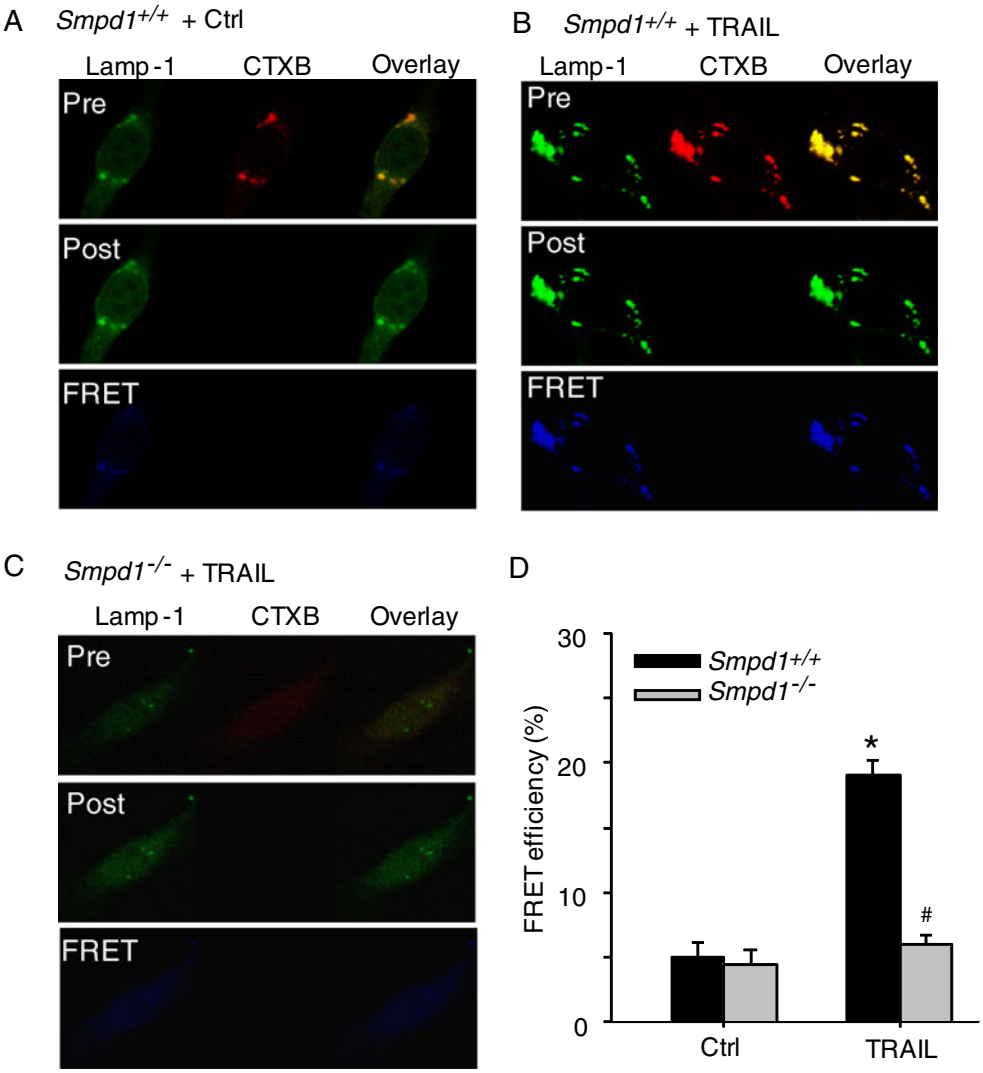

Fig. 6 TRAIL increases the expression of lysosome marker Lamp-1 in MR clusters in CAECs. **a**–**c** Representative confocal images of fluorescence resonance energy transfer (*FRET*) between FITC-Lamp-1 and TRITC-CTXB in $Smpd1^{+/+}$ CAECs treated with vehicle control (PBS buffer only) (**a**), TRAIL (**b**), or in $Smpd1^{-/-}$ CAECs with TRAIL (**c**). The FRET images were obtained by the subtraction of the pre-bleaching images from the post-bleaching images and shown in a *dark blue color*. Increased intensity of the blue color represents a higher level of FRET in these cells. **d** Displayed are the summarized data showing the effect of TRAIL on FRET efficiency between FITC-Lamp-1 and TRITC-CTXB in $Smpd1^{+/+}$ and $Smpd1^{-/-}$ CAECs. $^{*}P<0.05$ vs. $Smpd1^{+/+}$ control; $^{\#}P<0.05$ vs. $Smpd1^{+/+}$ TRAIL ($n=6$)

induced lysosome fusion requires ASM activity. Our findings are consistent with recent studies showing that ASM was required for the efficient phagolysosomal fusion [36, 37]. However, lysosomal fusion still occurs in ASM-deficient lymphoblasts, but endocytosis and plasma membrane repair were impaired in these cells [38]. Moreover, a recent study showing TCR-triggered fusion of lysosome-type lytic granules is not altered in ASM-deficient cytotoxic T lymphocytes compared to wild-type cells; in contrast, ASM deficiency results in an impaired expulsion of the vesicular contents [39]. Most recently, it has been demonstrated that oxidative stress triggered by H_2O_2 induces Ca^{2+}-dependent, but ASM-independent, lysosome fusion with the plasma membrane in Jurkat T cells [40]. It is possible that DR4 activation and H_2O_2 trigger different pathways to activate the ASM, for instance cleavage vs. oxidation, and that these different pathways also show a selective requirement of the ASM for the fusion process. Nonetheless, these studies suggest that the lysosome fusion process may involve ASM-dependent or ASM-independent mechanisms which depend on the cell types and the specific treatment used.

The present study did not attempt to further explore the precise mechanism of how ASM contributes to the lysosome fusion process in CAECs. It is possible that TRAIL induces a small amount of ceramide production (kindling ceramide) via the activation of ASM in the plasma membrane. This kindling ceramide may trigger lysosome trafficking and fusion to MR microdomains, which results in the translocation of more lysosomal ASM onto MRs, producing bonfire ceramide. Such bonfire ceramide may function as a driving force to promote MR clustering and the formation of important signaling platforms, which may further enhance lysosome trafficking and the fusion process [10, 41]. Nonetheless, this kindling and bonfire ceramide hypothesis in

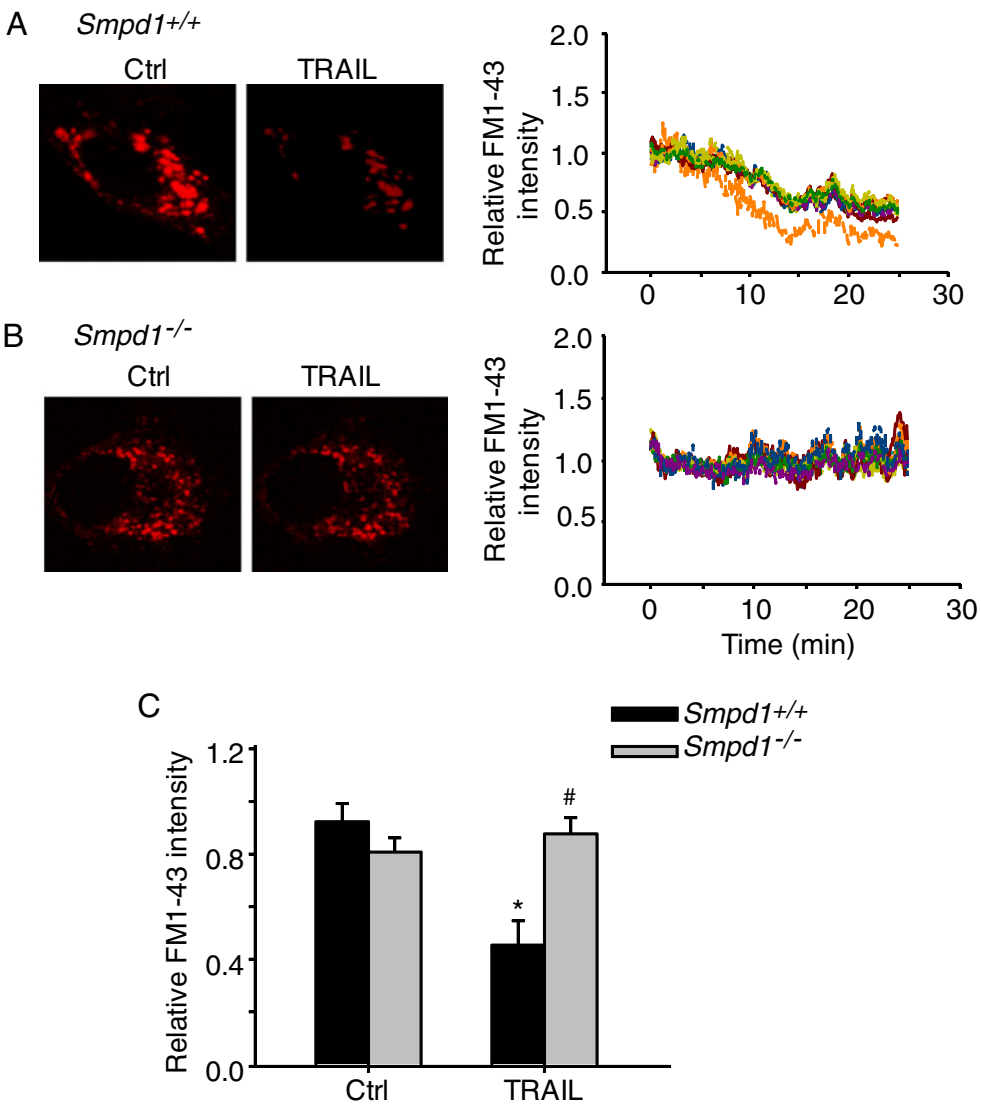

Fig. 7 Blockade of TRAIL-induced lysosome fusion with the plasma membrane in ASM-deficient CAECs. CAECs were first loaded with FM1-43, a lysosome-specific fluorescence probe, and then incubated in fresh medium containing BPB, which reversibly quenches FM1-43 fluorescence. In the quenching experiments, lysosome fusion with the plasma membrane will allow BPB to enter the lysosomes to quench FM1-43 fluorescence. **a** *Left panel*, Representative confocal fluorescence images of FM1-43 fluorescence in $Smpd1^{+/+}$ CAECs before and after treatment with TRAIL. *Right panel*, Representative traces of TRAIL-induced changes of FM1-43 fluorescence, normalized to that obtained before TRAIL treatment. **b** *Left panel*, Representative confocal fluorescence images of FM1-43 fluorescence quenching in $Smpd1^{-/-}$ CAECs treated with TRAIL. *Right panel*, Representative traces of TRAIL-induced changes of FM1-43 fluorescence in $Smpd1^{-/-}$ CAECs. **c** Summarized data showing the effect of TRAIL on FM1-43 fluorescence quenching in $Smpd1^{+/+}$ and $Smpd1^{-/-}$ CAECs. $^{*}P<0.05$ vs. $Smpd1^{+/+}$ control ($n=6$); $^{\#}P<0.05$ vs. $Smpd1^{+/+}$ TRAIL ($n=6$)

lysosome/MR-associated signaling needs to be tested in future studies.

In summary, the present study was the first to demonstrate that TRAIL is able to induce endothelial dysfunction as an early-stage acute action, which is associated with the assembly and activation of NADPH oxidase in MR clusters. The clustered MRs, together with the activated NADPH oxidase, constitute a redox signaling platform mediating the pathological actions of TRAIL on the vascular endothelium. Finally, we explored an essential role of ASM in the initiation of lysosome trafficking to and fusion with the plasma membrane in CAECs. The findings from the present study might increase our understanding of how MR redox signaling platforms are formed in ECs. Since death receptor ligands including TRAIL are implicated in the pathogenesis of various cardiovascular diseases such as atherosclerosis, the formation of the redox signaling platforms on the membrane of ECs may mediate the early response of the death receptors, leading to endothelial dysfunction in vivo and to the development of these diseases.

Acknowledgment This study was supported by grants from the National Institutes of Health (HL-57244, HL-075316, and HL-091464).

Disclosure of potential conflict of interests The authors declare no conflict of interests related to this study.

References

1. Schneider P, Bodmer JL, Thome M, Hofmann K, Holler N, Tschopp J (1997) Characterization of two receptors for TRAIL. FEBS Lett 416:329–334
2. Sheridan JP, Marsters SA, Pitti RM, Gurney A, Skubatch M, Baldwin D, Ramakrishnan L, Gray CL, Baker K, Wood WI et al

(1997) Control of TRAIL-induced apoptosis by a family of signaling and decoy receptors. Science 277:818–821
3. Emery JG, McDonnell P, Burke MB, Deen KC, Lyn S, Silverman C, Dul E, Appelbaum ER, Eichman C, DiPrinzio R et al (1998) Osteoprotegerin is a receptor for the cytotoxic ligand TRAIL. J Biol Chem 273:14363–14367
4. Secchiero P, Gonelli A, Carnevale E, Milani D, Pandolfi A, Zella D, Zauli G (2003) TRAIL promotes the survival and proliferation of primary human vascular endothelial cells by activating the Akt and ERK pathways. Circulation 107:2250–2256
5. Secchiero P, Corallini F, di Iasio MG, Gonelli A, Barbarotto E, Zauli G (2005) TRAIL counteracts the proadhesive activity of inflammatory cytokines in endothelial cells by down-modulating CCL8 and CXCL10 chemokine expression and release. Blood 105:3413–3419
6. Fossati S, Ghiso J, Rostagno A (2012) TRAIL death receptors DR4 and DR5 mediate cerebral microvascular endothelial cell apoptosis induced by oligomeric Alzheimer's Abeta. Cell Death Dis 3:e321
7. Li JH, Kirkiles-Smith NC, McNiff JM, Pober JS (2003) TRAIL induces apoptosis and inflammatory gene expression in human endothelial cells. J Immunol 171:1526–1533
8. Alladina SJ, Song JH, Davidge ST, Hao C, Easton AS (2005) TRAIL-induced apoptosis in human vascular endothelium is regulated by phosphatidylinositol 3-kinase/Akt through the short form of cellular FLIP and Bcl-2. J Vasc Res 42:337–347
9. Zhang Y, Li X, Becker KA, Gulbins E (2009) Ceramide-enriched membrane domains—structure and function. Biochim Biophys Acta 1788:178–183
10. Grassme H, Jekle A, Riehle A, Schwarz H, Berger J, Sandhoff K, Kolesnick R, Gulbins E (2001) CD95 signaling via ceramide-rich membrane rafts. J Biol Chem 276:20589–20596
11. Zhang AY, Yi F, Zhang G, Gulbins E, Li PL (2006) Lipid raft clustering and redox signaling platform formation in coronary arterial endothelial cells. Hypertension 47:74–80
12. Dupree JL, Pomicter AD (2010) Myelin, DIGs, and membrane rafts in the central nervous system. Prostaglandins Other Lipid Mediat 91:118–129
13. Natoli G, Costanzo A, Guido F, Moretti F, Levrero M (1998) Apoptotic, non-apoptotic, and anti-apoptotic pathways of tumor necrosis factor signalling. Biochem Pharmacol 56:915–920
14. Zhang AY, Yi F, Jin S, Xia M, Chen QZ, Gulbins E, Li PL (2007) Acid sphingomyelinase and its redox amplification in formation of lipid raft redox signaling platforms in endothelial cells. Antioxid Redox Sig 9:817–828
15. Jin S, Zhang Y, Yi F, Li PL (2008) Critical role of lipid raft redox signaling platforms in endostatin-induced coronary endothelial dysfunction. Arterioscler Thromb Vasc Biol 28:485–490
16. Bao JX, Xia M, Poklis JL, Han WQ, Brimson C, Li PL (2010) Triggering role of acid sphingomyelinase in endothelial lysosome-membrane fusion and dysfunction in coronary arteries. Am J Physiol Heart Circ Physiol 298:H992–H1002
17. Bao JX, Jin S, Zhang F, Wang ZC, Li N, Li PL (2010) Activation of membrane NADPH oxidase associated with lysosome-targeted acid sphingomyelinase in coronary endothelial cells. Antioxid Redox Sig 12:703–712
18. Dumitru CA, Gulbins E (2006) TRAIL activates acid sphingomyelinase via a redox mechanism and releases ceramide to trigger apoptosis. Oncogene 25:5612–5625
19. Teng B, Ansari HR, Oldenburg PJ, Schnermann J, Mustafa SJ (2006) Isolation and characterization of coronary endothelial and smooth muscle cells from A1 adenosine receptor-knockout mice. Am J Physiol Heart Circ Physiol 290:H1713–H1720
20. Li JM, Mullen AM, Shah AM (2001) Phenotypic properties and characteristics of superoxide production by mouse coronary microvascular endothelial cells. J Mol Cell Cardiol 33:1119–1131
21. Boini KM, Xia M, Li C, Zhang C, Payne LP, Abais JM, Poklis JL, Hylemon PB, Li PL (2011) Acid sphingomyelinase gene deficiency ameliorates the hyperhomocysteinemia-induced glomerular injury in mice. Am J Pathol 179:2210–2219
22. Jin S, Yi F, Zhang F, Poklis JL, Li PL (2008) Lysosomal targeting and trafficking of acid sphingomyelinase to lipid raft platforms in coronary endothelial cells. Arterioscler Thromb Vasc Biol 28:2056–2062
23. Zhang DX, Yi FX, Zou AP, Li PL (2002) Role of ceramide in TNF-alpha-induced impairment of endothelium-dependent vasorelaxation in coronary arteries. Am J Physiol Heart Circ Physiol 283:H1785–H1794
24. Bellail AC, Tse MC, Song JH, Phuphanich S, Olson JJ, Sun SY, Hao C (2010) DR5-mediated DISC controls caspase-8 cleavage and initiation of apoptosis in human glioblastomas. J Cell Mol Med 14:1303–1317
25. Song JH, Tse MC, Bellail A, Phuphanich S, Khuri F, Kneteman NM, Hao C (2007) Lipid rafts and nonrafts mediate tumor necrosis factor related apoptosis-inducing ligand induced apoptotic and nonapoptotic signals in non small cell lung carcinoma cells. Cancer Res 67:6946–6955
26. Xu L, Qu X, Zhang Y, Hu X, Yang X, Hou K, Teng Y, Zhang J, Sada K, Liu Y (2009) Oxaliplatin enhances TRAIL-induced apoptosis in gastric cancer cells by CBL-regulated death receptor redistribution in lipid rafts. FEBS Lett 583:943–948
27. Rossin A, Derouet M, Abdel-Sater F, Hueber AO (2009) Palmitoylation of the TRAIL receptor DR4 confers an efficient TRAIL-induced cell death signalling. Biochem J 419:185–192
28. Goni FM, Alonso A (2000) Membrane fusion induced by phospholipase C and sphingomyelinases. Biosci Rep 20:443–463
29. Min Y, Shi J, Zhang Y, Liu S, Liu Y, Zheng D (2009) Death receptor 5-recruited raft components contributes to the sensitivity of Jurkat leukemia cell lines to TRAIL-induced cell death. IUBMB Life 61:261–267
30. Yang B, Rizzo V (2007) TNF-alpha potentiates protein-tyrosine nitration through activation of NADPH oxidase and eNOS localized in membrane rafts and caveolae of bovine aortic endothelial cells. Am J Physiol Heart Circ Physiol 292:H954–H962
31. Shao D, Segal AW, Dekker LV (2003) Lipid rafts determine efficiency of NADPH oxidase activation in neutrophils. FEBS Lett 550:101–106
32. Samhan-Arias AK, Garcia-Bereguiain MA, Martin-Romero FJ, Gutierrez-Merino C (2009) Clustering of plasma membrane-bound cytochrome b5 reductase within 'lipid raft' microdomains of the neuronal plasma membrane. Mol Cell Neurosci 40:14–26 D
33. Zauli G, Pandolfi A, Gonelli A, Di Pietro R, Guarnieri S, Ciabattoni G, Rana R, Vitale M, Secchiero P (2003) Tumor necrosis factor-related apoptosis-inducing ligand (TRAIL) sequentially upregulates nitric oxide and prostanoid production in primary human endothelial cells. Circ Res 92:732–740
34. Di Pietro R, Mariggio MA, Guarnieri S, Sancilio S, Giardinelli A, Di Silvestre S, Consoli A, Zauli G, Pandolfi A (2006) Tumor necrosis factor-related apoptosis-inducing ligand (TRAIL) regulates endothelial nitric oxide synthase (eNOS) activity and its localization within the human vein endothelial cells (HUVEC) in culture. J Cell Biochem 97:782–794
35. Heylen E, Huang A, Sun D, Kaley G (2009) Nitric oxide-mediated dilation of arterioles to intraluminal administration of aldosterone. J Cardiovasc Pharmacol 54:535–542
36. Schramm M, Herz J, Haas A, Kronke M, Utermohlen O (2008) Acid sphingomyelinase is required for efficient phago-lysosomal fusion. Cell Microbiol 10:1839–1853
37. Utermohlen O, Herz J, Schramm M, Kronke M (2008) Fusogenicity of membranes: the impact of acid sphingomyelinase on innate immune responses. Immunobiology 213:307–314
38. Tam C, Idone V, Devlin C, Fernandes MC, Flannery A, He X, Schuchman E, Tabas I, Andrews NW (2010) Exocytosis of acid

sphingomyelinase by wounded cells promotes endocytosis and plasma membrane repair. J Cell Biol 189:1027–1038
39. Herz J, Pardo J, Kashkar H, Schramm M, Kuzmenkina E, Bos E, Wiegmann K, Wallich R, Peters PJ, Herzig S et al (2009) Acid sphingomyelinase is a key regulator of cytotoxic granule secretion by primary T lymphocytes. Nat Immunol 10:761–768
40. Li X, Gulbins E, Zhang Y (2012) Oxidative stress triggers Ca-dependent lysosome trafficking and activation of acid sphingomyelinase. Cell Physiol Biochem 30:815–826
41. Yu C, Alterman M, Dobrowsky RT (2005) Ceramide displaces cholesterol from lipid rafts and decreases the association of the cholesterol binding protein caveolin-1. J Lipid Res 46:1678–1691